## NUCLEAR EXPERIMENTAL TECHNIQUES

# A Radiographic Facility for the 70-GeV Proton Accelerator of the Institute for High Energy Physics

**Yu. M. Antipov[a], A. G. Afonin[a], A. V. Vasilevskii[†a], I. A. Gusev[a], V. I. Demyanchuk[a], O. V. Zyat'kov[a],
N. A. Ignashin[a], Yu. G. Karshev[†a], A. V. Larionov[a], A. V. Maksimov[a], A. A. Matyushin[a],
A. V. Minchenko[a], M. S. Mikheev[a], V. A. Mirgorodskii[a], V. N. Peleshko[a], V. D. Rud'ko[a],
V. I. Terekhov[a], N. E. Tyurin[a], Yu. S. Fedotov[a], Yu. A. Trutnev[b], V. V. Burtsev[b], A. A. Volkov[b],
I. A. Ivanin[b], S. A. Kartanov[b], Yu. P. Kuropatkin[b], A. L. Mikhailov[b], K. L. Mikhailyukov[b],
O. V. Oreshkov[b], A. V. Rudnev[b], G. M. Spirov[b], M. A. Syrunin[b],
M. V. Tatsenko[b], I. A. Tkachenko[b], and I. V. Khramov[b]**

[a] *Institute for High Energy Physics, ul. Pobedy 1, Protvino, Moscow oblast, 142281 Russia*
[b] *All-Russia Research Institute of Experimental Physics, Russian Federal Nuclear Center,
pr. Mira 37, Sarov, Nizhni Novgorod oblast, 607188 Russia*
Received September 1, 2009

**Abstract**—A radiographic facility for the 70-GeV proton accelerator of the Institute for High Energy Physics is described. The available infrastructure in the initial straight part of the injection channel is used in the facility. The 100-mm-diameter lenses of the injection line are intended for transportation of the proton beam from the U-70 accelerator to the accelerating–storage complex. The facility has been designed only for an energy of 50 GeV with a viewfield of 60 mm and used for imaging of samples with an optical density of >300 g/cm$^2$ in the presence of some losses in the line. The optical resolution of the facility is 0.25 mm. A set of experiments aimed at multiframe recording of fast processes were conducted on the facility in 2004–2008. Small-sized explosion-proof chambers, as well as the measuring system for monitoring the state of the chamber and environment, were used in the dynamic experiments.

## INTRODUCTION

Over more than half a century, flash X-ray radiography has been the basic tool for studying fast processes. The wide application of X-ray radiography can be explained by its advantages, such as the simplicity of the method and the relative cheapness of the facilities, the main component of which is an electron accelerator.

Many problems inherent in the flash X-ray radiography are absent in the proton radiography. The mean free path of high-energy protons is ~185 g/cm$^2$. At an optical density of ~300 g/cm$^2$, approximately 20% of protons pass through the sample (by contrast to $10^{-6}$ for γ rays). Therefore, the quantity of protons millions of times smaller than that of γ rays is required for formation of an X-ray radiographic image. A proton being a charged particle allows one to control directed radiation fluxes in order to perform multiframe and multibeam imaging based on a single accelerator. The use of two sets of detectors offers a unique chance to determine charge $Z$ and atomic mass $A$ of a substance at any point of the analyzed sample. Incidentally, the mass concentrations of substances can also be determined.

The availability of protons with energies of 50–70 GeV is the main requirement of proton radiography. Energies as high as these are needed for examining an optically thick object to its full depth and, which is more important, for obtaining high-definition images, since an increase in the proton energy leads to a decrease in image blurring by chromatic aberrations and multiple Coulomb scattering. The use of special magnetic optics makes it possible to substantially reduce the effect of Coulomb scattering and obtain an optical resolution of better than 1 mm for samples with an optical density of >300 g/cm$^2$.

The availability of both the 70-GeV proton accelerator (U-70) and an advanced beam extraction system at the Institute for High Energy Physics (IHEP) provides a means for using the accelerator to examine samples with any required thickness by the proton radiography method.

In 2003, Yu.A. Trutnev and O.V. Oreshkov, the staff members at the All-Russia Research Institute of Experimental Physics, in common with N.E. Tyurin and Y.S. Fedotov, the staff members at the IHEP, sug-
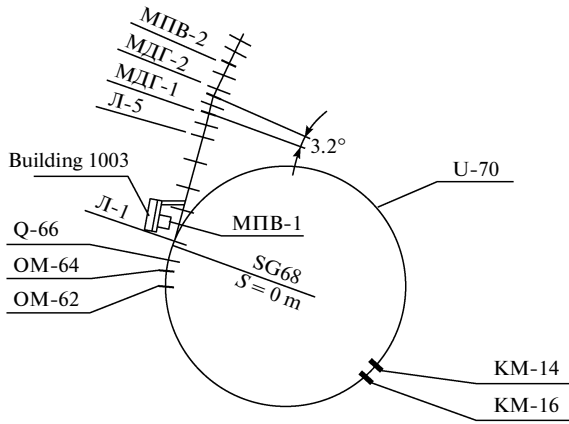
---

† Deceased.

**Fig. 1.** Schematic diagram of the U-70 accelerator ring at the entrance into the injection line: (U-70) accelerator ring, (KM-14, KM-16) kicker magnets located in the straight gaps SG14 and SG16 of the accelerator, (OM-62, OM-64) extraction magnets located in the straight gaps SG62 and SG64 of the accelerator, (Q-66) lens for preliminary focusing of the proton beam in the SG66, (Л-1—Л-5) IL lenses, (МПВ-1, МПВ-2) bending vertical magnets, and (МДГ-1, МДГ-2) dispersion horizontal magnets; the IL input is in the SG68.

gested to create a radiographic facility for the 70-GeV accelerator of the IHEP. This task was practically performed at the IHEP by the joint efforts of two research centers—the IHEP and the All-Russia Research Institute of Experimental Physics—in 2004–2008. Static and dynamic experiments were carried out on the U-70 proton beams using test objects differing in the complexity, and the capabilities of the proton radiography technique were experimentally demonstrated.

In this paper, we describe the design of the optical and electronic systems that have made it possible to obtain these results.

## CHARACTERISTICS OF THE PROTON SYNCHROTRON AT THE IHEP

The U-70 accelerating complex [1] at the IHEP comprises the 30-MeV URAL-30 linear accelerator, a

1.5-GeV fast-cycling booster, and a 70-GeV proton synchrotron. The maximum intensity of the 70-GeV proton beam is $\sim 1.7 \times 10^{13}$ particles per spill. The total duration of a magnetic cycle during acceleration to 70 GeV is $\sim 10$ s at a 2-s duration of the magnetic field plateau at maximum energy. The booster can inject 3–29 proton bunches to the U-70 orbit. The minimum particle intensity in the bunch sufficient for stable operation of the feedback system is $3 \times 10^{11}$ particles. The fast extraction system [2] allows extraction of 1–29 bunches once per cycle. Therefore, the minimum intensity in a spill is $3 \times 10^{11}$ protons, and the maximum intensity is as high as $1.5 \times 10^{13}$ protons. The emittance of the accelerated beam at the maximum intensity is 2 mm mrad; at a lower intensity, its value may be $\sim 1$ mm mrad. The duration of a bunch is 20–30 ns (95%) at a high intensity and can be reduced to 5 ns by applying special procedures to the accelerating system.

## ARRANGEMENT OF THE EXPERIMENTAL FACILITY

The optical system is the heart of the proton radiographic facility developed on the basis of the available infrastructure—the injection line (IL) [3]. The optical system is composed of four quadrupole lenses (a quartet) and has a transfer matrix of −1 for the horizontal and vertical planes of the transverse motion [4]. It is the straight initial segment of the IL on which a single magnetooptical quartet with a matrix of −1 can be built (Fig. 1). The IL quadrupole magnets with a diameter of 100 mm, length $l_1 = 1$ m, and maximum gradient of the magnetic field $G_1 = 1.3$ kG/cm are used as the quartet lenses. The quadrupole power is

$$K_{1(70)} = \frac{G_1 l_1}{B_{0(70)} R_0} = 5.58 \times 10^{-2} \ \text{m}^{-1}$$

for a 70-GeV beam and

$$K_{1(50)} = \frac{G_1 l_1}{B_{0(50)} R_0} = 7.79 \times 10^{-2} \ \text{m}^{-1}$$

for a 50-GeV beam, where $B_{0(70)} R_0 = 2329.5$ kG m and $B_{0(50)} R_0 = 1667.5$ kG m are the magnetic rigidities of the proton beam at 70 and 50 GeV, respectively.
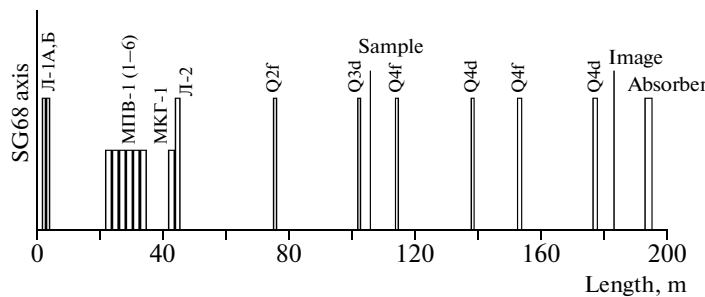


**Fig. 2.** The optical scheme of the irradiating facility: (Л-1А, Б, Л-2) IL lens, (МКГ-1) horizontal correction magnet, (Q2f, Q3d) lenses for forming the proton beam on the sample, and (Q4f—Q4d—Q4f—Q4d) lenses of the quartet.
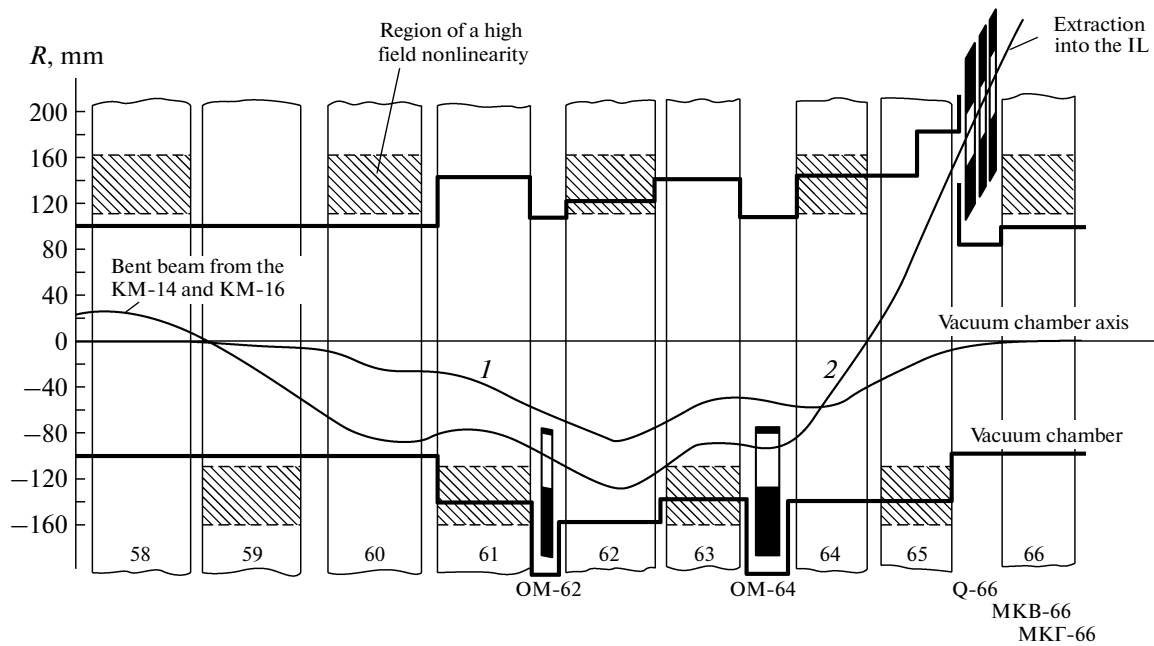
**Fig. 3.** Diagram of proton beam extraction into the IL: (OM-62, OM-64) extraction magnets, (Q-66) lens for preliminary focusing of the proton beam, and (МКВ-66, МКГ-66) vertical and horizontal beam-positioning magnets, respectively.

Using a thin-lens approximation, we find the respective lengths of the quartets for two energies:

$$L_{(70)} = \frac{4\sqrt{2}}{K_{1(70)}} = 101.4 \text{ m} \text{ and } L_{(50)} = \frac{4\sqrt{2}}{K_{1(50)}} = 72.6 \text{ m}.$$

The length of the straight IL segment from straight gap 68 (SG68) to the МДГ-1 bending magnet is ~210 m, and the length of the forming segment is ~110 m. It is the straight IL segment where the quartet of quadrupoles for a sole energy of 50 GeV has been installed (Fig. 2).

The optical schematic diagram of the facility looks as follows: lenses Л-3 and Л-4 are replaced by lenses Q2f and Q3d on the segment where the proton beam directed toward the object is formed, and lenses Q4f–Q4d–Q4f–Q4d form a quartet with a transfer matrix of −1 for two planes of motion.

## EXTRACTION OF THE PROTON BEAM TOWARD THE FACILITY

An accelerated proton beam is extracted into the IL by the fast extraction system, the first component of which is the KM-16 fast kicker magnet. The beam
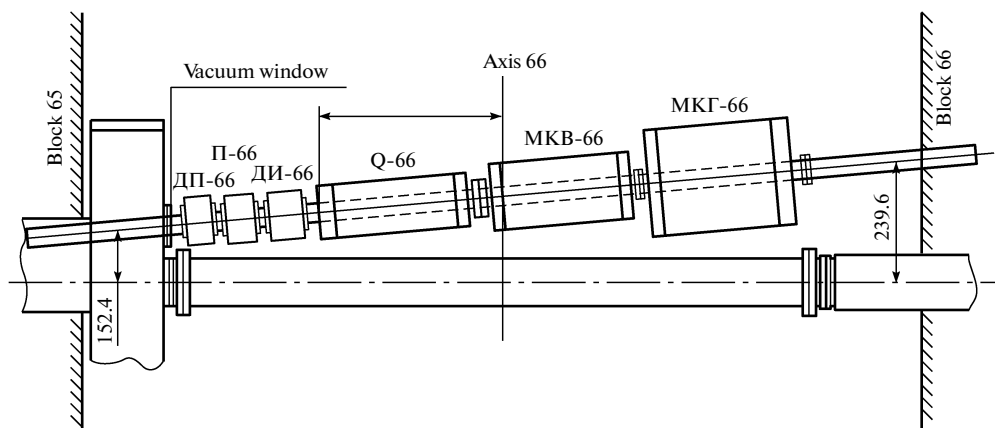


**Fig. 4.** Arrangement of the extraction equipment in the SG66: (ДП-66) sensor for measuring the center of gravity of the proton beam, (П-66) beam profile monitor, (ДИ-66) intensity meter, (Q-66) lens for preliminary focusing of the proton beam, and (МКВ-66, МКГ-66) vertical and horizontal beam-positioning magnets, respectively.
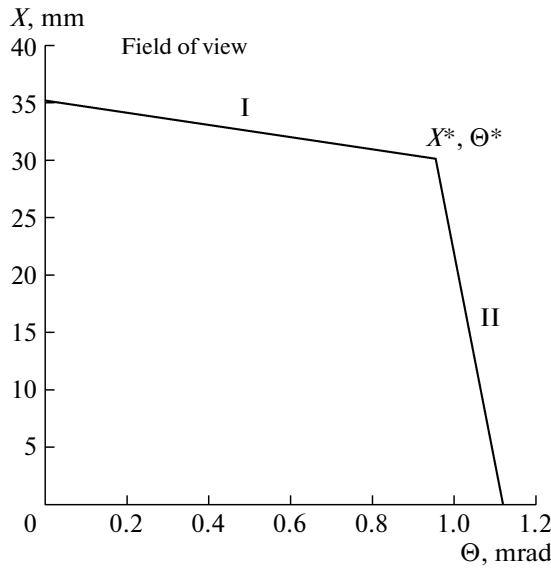
**Fig. 5.** Field of view of the quartet at a beam energy of 50 GeV: ($X$) radius of the field of view, and ($\Theta$) is the scattering angle for protons in the sample material.



**Fig. 6.** Proton radiography snapshot of the cumulative jet formation process.

bent by the KM-16 magnet is guided to the OM-62 and OM-64 extraction magnets (see Fig. 1). A preliminary beam shift toward the extraction magnets is attained by a local bump of the closed orbit (trajectory *1* in Fig. 3). These magnets eject the beam out of the vacuum chamber of the accelerator into the 66th straight gap (SG66, trajectory *2* in Fig. 3). In this gap, there are the Q-66 preliminary focusing lens, MKB-66 beam-positioning magnet of the vertical plane of motion, МКГ-66 beam-positioning magnet of the horizontal plane of motion, ДП-66 beam position monitor in the radial plane of motion, П-66 profile monitor used to measure the profiles of the extracted beam cross sections in the radial and vertical planes, and ДИ-66 intensity meter of the extracted beam (Fig. 4).

## IRRADIATION OF A SAMPLE AND FORMATION OF ITS IMAGE

At the focal point, the matrix of the one-half of the quartet (i.e., the doublet) with lens powers $K_{1(50)}$, which defines the structure functions of the quartet, is

$$M_{db} = \begin{pmatrix} \alpha_0 & \beta_0 \\ -\gamma_0 & -\alpha_0 \end{pmatrix} = \begin{pmatrix} -1.82177 & 31.66147 \\ -0.13641 & 1.82177 \end{pmatrix},$$

where $\alpha_0, \beta_0, \gamma_0$ are the Twiss parameters.

The slope of the ellipse—the quartet's acceptance—is

$$W_0 = -\frac{\alpha_0}{\beta_0} = 0.057539 \text{ m}^{-1}.$$

The emittances of the irradiating beam in the radial and vertical planes are $\varepsilon_{r,z} = 2 \times 10^{-6}$ m rad. The radius

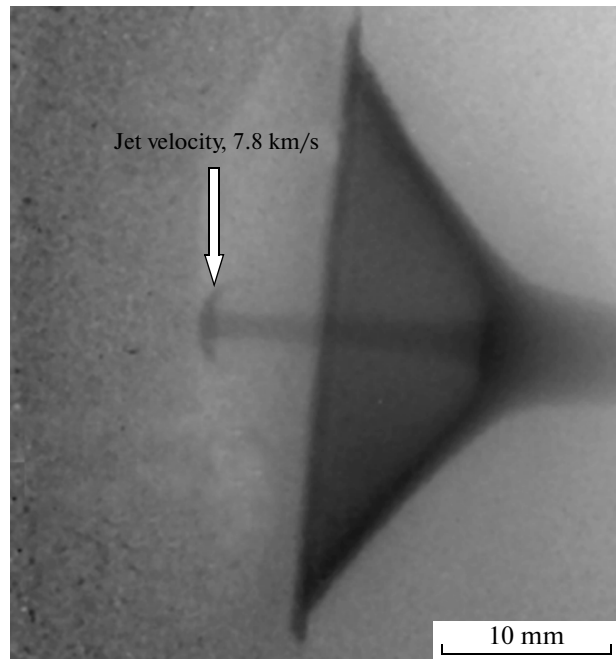of the irradiating beam is selected to be (see Fig. 5) $A_{r,z} = 30$ mm. Therefore, the beam parameters are

$$\beta_{r,z\,\text{beam}} = \frac{A_{r,z}^2}{\varepsilon_{r,z}} = 450 \text{ m},$$

$$\alpha_{r,z\,\text{beam}} = \mp\beta_{r,z\,\text{beam}}W = \mp25.89,$$

where $\beta_{r,z\,\text{beam}}$ characterizes the envelope, and $\alpha_{r,z\,\text{beam}}$ is the slope of the irradiating-beam ellipse.

It is these values that must be attained with the extracted beam at the sample.

The allowable increase in the beam passing lossless through the lens quartet is governed by its acceptance. The scattering value of the irradiating beam depends on the radiation length of the material and thickness of the sample. For the maximum field of view to be obtained, the emittance of the irradiating beam must be matched to its acceptance by obtaining the slope of the beam's phase ellipse such that it is equal to the slope of the quartet's acceptance:

$$W_0 = -\frac{\alpha_0}{\beta_0} = \frac{x'_{\text{max}}}{x_{\text{max}}},$$

where angle $x'_{\text{max}}$ corresponds to a particle with maximum offset $x_{\text{max}}$.

Using matrices of segments I and II from the entrance into the quartet to the focusing lenses, we obtain expressions for two straight lines that limit the field of view (Fig. 5):

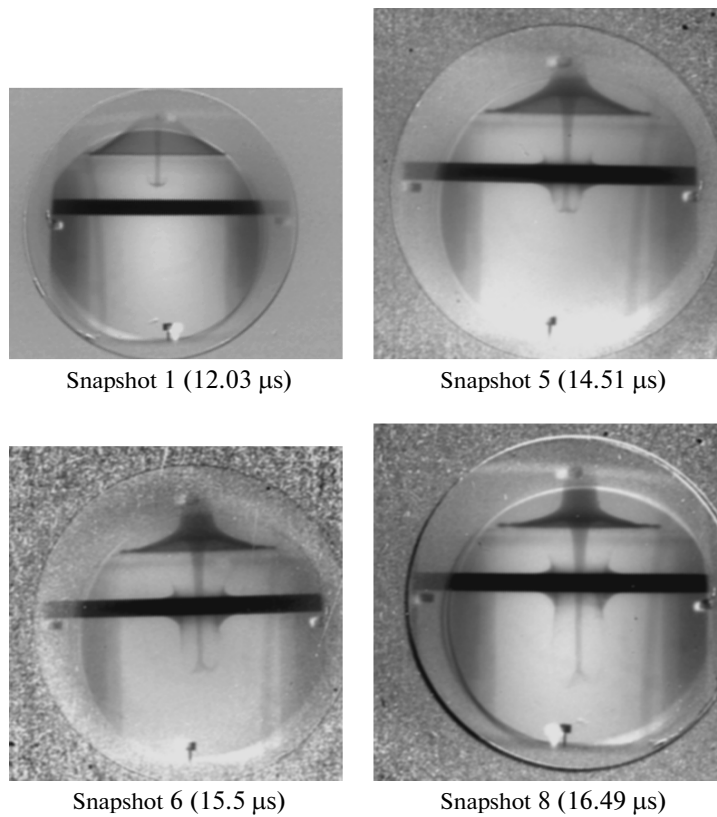$$\text{I—}X_{\text{vf}} = 0.68R_{\text{ch}} - \frac{0.48}{K_1}\Theta_{\text{sc}},$$

Snapshot 1 (12.03 μs)



Snapshot 5 (14.51 μs)



Snapshot 6 (15.5 μs)



Snapshot 8 (16.49 μs)

**Fig. 7.** Proton radiography snapshot of the cumulative jet affecting the thin plate.

$$\text{II}—X_{\mathrm{vf}} = 3R_{\mathrm{ch}} - \frac{10.22}{K_1}\Theta_{\mathrm{sc}},$$

where $R_{\mathrm{ch}}$ is the radius of the vacuum chamber in the quadrupole lens, and $\Theta_{\mathrm{sc}}$ is the angle of scattering in the sample material.

The point of intersection of these straight lines with coordinates

$$X^* = 0.56R_{\mathrm{ch}}, \quad \Theta^* = 0.24R_{\mathrm{ch}}K_1$$

is the characteristic point in the behavior of the field of view as a function of the scattering angle.

Figure 5 demonstrates that a high-quality image can be obtained on this facility if the diameter of the test object is <60 mm. The distribution of the proton beam scattered in the substance is assumed to be the Gaussian function with the rms scattering angle

$$\sigma_{\mathrm{sc}} = \frac{13.6}{p\beta}\sqrt{\frac{L}{L_R}},$$

where $p$ [MeV/$c$] is the proton momentum, $\beta$ is the proton velocity in terms of the velocity of light, $L$ is the thickness of the irradiated sample, and $L_R$ is the radiation length of the sample material. Therefore, for 95% beam content in angle $\Theta_{\mathrm{sc}} = 2\sigma_{\mathrm{sc}}$, the length of a lead sample that can be irradiated without losses of the beam on the walls of the vacuum chamber is $\cong$20 mm. Assuming that some losses of the proton beam exist,

one can obtain a high-quality image of a sample up to 350 mm in length.

## EXPERIMENTAL BEAMLINE

The analyzed sample is placed at the input of the quartet, and the system for recording its image is installed at its output. A device for automatic change of collimators, which is shaped as a 500-mm-diameter drum, is located at the focal point of the quartet. In the drum, there are eight positions for placing collimators of different types and diameters and a high-precision instrument for measuring the center of gravity of the proton beam. This device allows the required collimator to be rapidly installed without vacuum deterioration in the beamline.

A "friendly" interface has been developed to control the facility. It allows one to turn the facility on or off, set the required currents in the magnetooptical components of the beamline, measure the currents in individual components and in the vacuum pumps, and take readings of the beam diagnostic devices.

Proton radiography images were recorded by means of a modular multiframe electron-optical recording system based on CCD arrays, which currently allows obtaining of as many as 29 independent snapshots with an image field diameter of up to ~60 mm and a radiographing time interval of up to
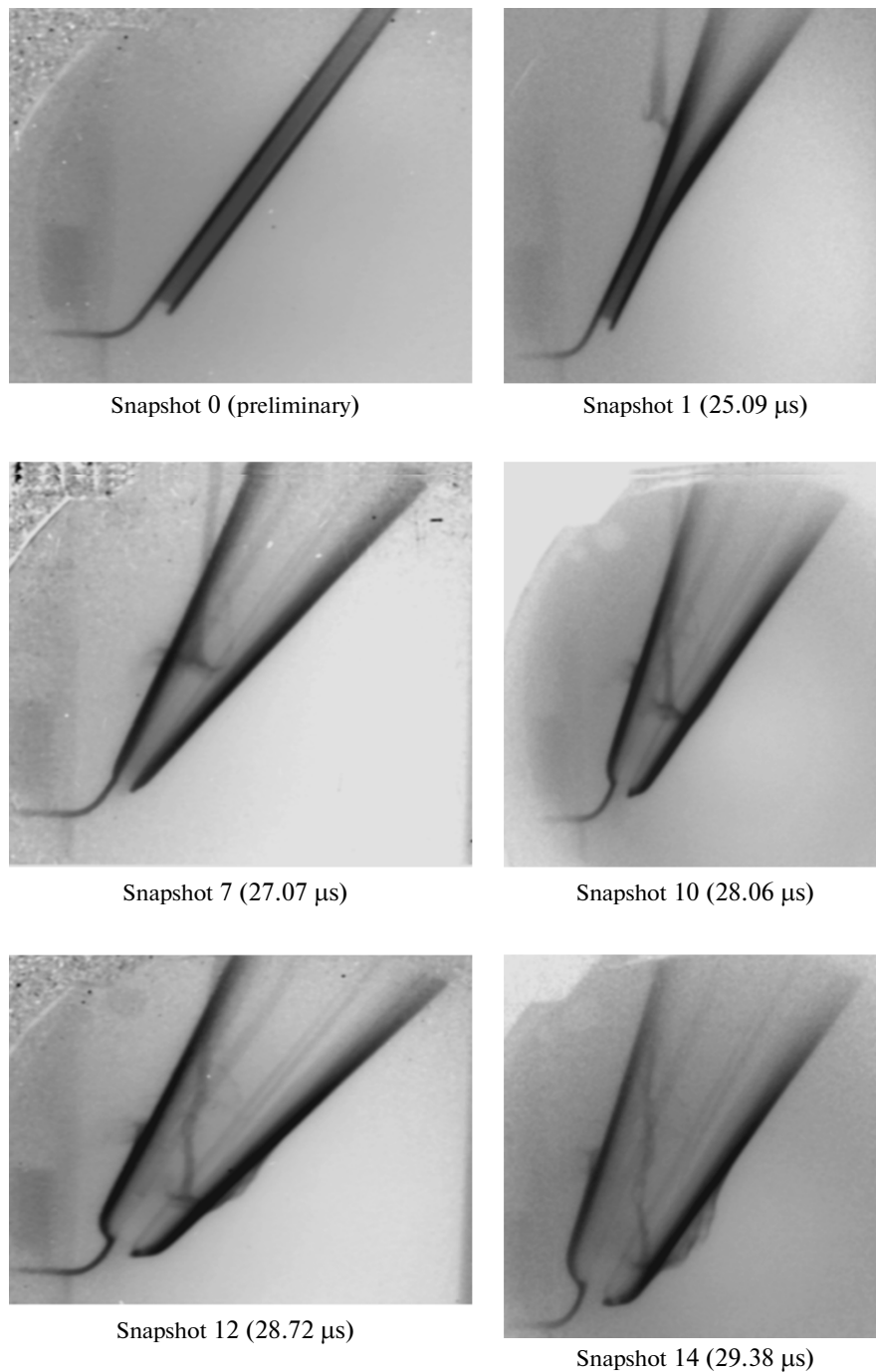
Snapshot 0 (preliminary)

Snapshot 1 (25.09 μs)

Snapshot 7 (27.07 μs)

Snapshot 10 (28.06 μs)

Snapshot 12 (28.72 μs)

Snapshot 14 (29.38 μs)

**Fig. 8.** Proton radiography snapshot of the interaction between the cumulative jet and the sandwich wall composed of two steel plates separated by a layer of an explosive material.

~5 μs (with a minimum time between snapshots of 165 ns and an exposure time of 10–30 ns). Several types of small-sized explosion-proof chambers capable of localizing the energy release to a level of ~2.5 kg of trinitrotoluene equivalent, as well as the measuring system for monitoring the state of the chamber and environment, were used in the dynamic experiments in the IL of the accelerating complex.

Figures 6–10 present the examples of proton radiography multiframe images of dynamic processes: formation of a cumulative jet ~2 mm in diameter (Fig. 6), effect of the cumulative jet on the steel plate (Fig. 7) and the sandwich wall composed of two steel plates with an explosive material placed between them (Fig. 8), development of the Rayleigh–Taylor instability upon loading a copper liner with predetermined
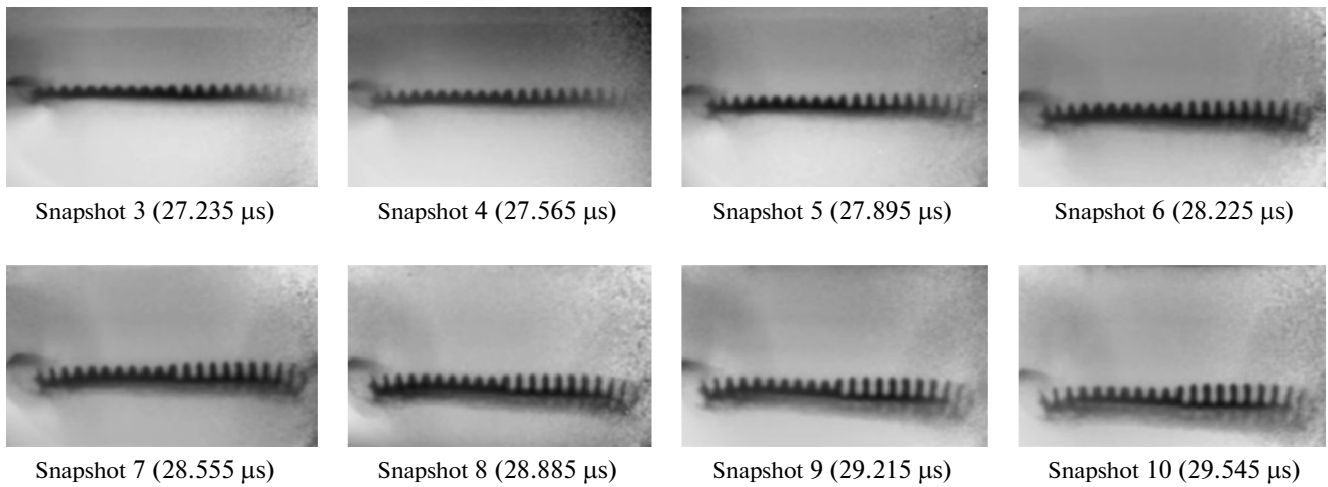
Snapshot 3 (27.235 μs)      Snapshot 4 (27.565 μs)      Snapshot 5 (27.895 μs)      Snapshot 6 (28.225 μs)

Snapshot 7 (28.555 μs)      Snapshot 8 (28.885 μs)      Snapshot 9 (29.215 μs)      Snapshot 10 (29.545 μs)

**Fig. 9.** Proton radiography snapshot of the Rayleigh–Taylor instability process; the initial perturbations are 4 μm in the left part and 8 μm in the right part of the liner.
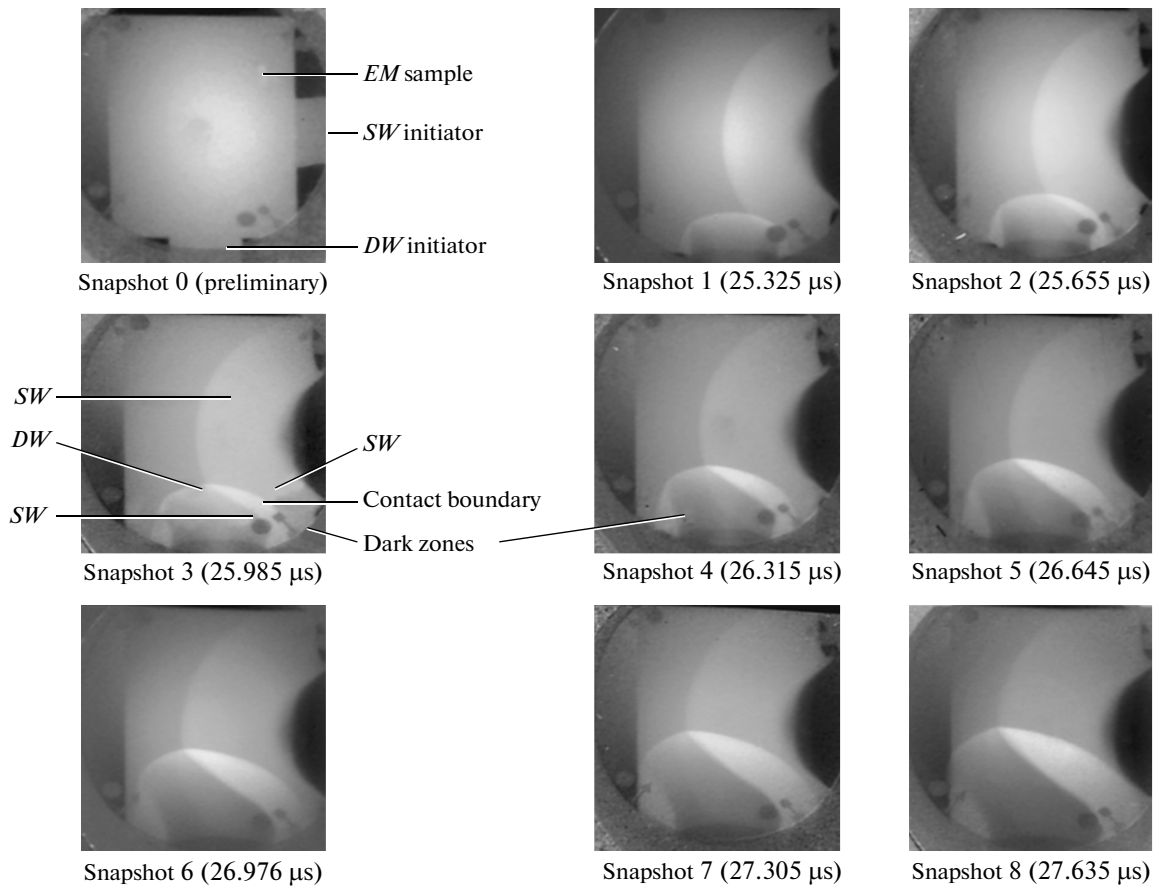


Snapshot 0 (preliminary)      Snapshot 1 (25.325 μs)      Snapshot 2 (25.655 μs)

Snapshot 3 (25.985 μs)      Snapshot 4 (26.315 μs)      Snapshot 5 (26.645 μs)

Snapshot 6 (26.976 μs)      Snapshot 7 (27.305 μs)      Snapshot 8 (27.635 μs)

**Fig. 10.** Proton radiography snapshot of the interaction between the shock and detonation waves from an explosive material: (*SW*) shock wave, (*DW*) detonation wave, and (*EM*) explosive material.

initial perturbations by a pressure of up to ≈55 GPa (Fig. 9) [5], and interaction of the detonation and shock waves as they propagate in the sample of explosive material (Fig. 10) [6]. On the snapshots of proton radiography images, time is counted from the instant of initiation.

## CONCLUSIONS

A unique proton radiography irradiation facility capable of forming images of samples with a diameter of 60 mm and an optical (mass) thickness of >300 g/cm² at an energy of 50 GeV has been developed by the IHEP with the use of the available infrastructure. The optical resolution of this facility is 0.25 mm. The ways for improving the parameters of the proton beam and the facility are currently being considered.

## REFERENCES

1. Ado, Yu.M., Zhuravlev, A.A., Logunov, A.A., et al., *At. Energ.*, 1970, vol. 28, no. 2, p. 132.

2. Myznikov, K.P., Tatarenko, V.M., Fedotov, Yu.S., et al.,, *Preprint of Inst. for High Energy Phys.*, Protvino, 1968, no. 68-57-K, p. 14.

3. Baranov, V.T., Tatarenko, V.M., Fedotov, Yu.S., et al., *Preprint of Inst. for High Energy Phys.*, Protvino, 1992, no. 92-118, p. 24.

4. Mottershead C.T. and Zumbro J.D., *Preprint of LANL*, Los Alamos, New Mexico, 1998, no. 87545, p. 12.

5. Igonin, V.V., Lebedev, A.I., Nizovtsev, P.N., et al., *Proc. of the 7th International Workshop on the Physics of Compressible Turbulent Mixing*, St. Peterburg, 1999, p. 171.

6. Morozov, V.G., Karpenko, I.I., Kuratov, S.E., et al., *Khim. Fiz.*, 1995, vol. 14, nos. 2−3, p. 32.